J. Phys. Chem. A **2000,** *104,* 801−810

Selected Ion Flow Tube Studies of $S^+(^4S)$ Reactions with Small Oxygenated and Sulfurated Organic Molecules

Brian K. Decker, Lucia M. Babcock, and Nigel G. Adams*

Department of Chemistry, The University of Georgia, Athens, Georgia 30602

Received: July 20, 1999; In Final Form: November 11, 1999

The reactions of ground-state $S^+(^4S)$ with CH_3OH, CH_3SH, C_2H_5OH, C_2H_5SH, CH_3OCH_3, CH_3SCH_3, CH_2O, CH_3CHO, C_2H_5CHO, $CH_3C(O)CH_3$, $C_2H_5C(O)CH_3$, HCO_2H, CH_3CO_2H, $C_2H_5CO_2H$, HCO_2CH_3, $HCO_2C_2H_5$, $CH_3CO_2CH_3$, $CH_3CO_2C_2H_5$, $C_2H_5CO_2CH_3$, and $C_2H_5CO_2C_2H_5$ have been studied with a selected ion flow tube (SIFT) at 296 ± 4 K. All of these reactions proceed rapidly, with binary rate coefficients $\geq {}^2/_3 k_{th}^{(2)}$, where $k_{th}^{(2)}$ is the theoretical binary collisional rate coefficient. A strong correlation between the exothermicity of charge (i.e., electron) transfer and the prominence of the charge-transfer channel is observed. Extensive branching into numerous product channels occurs in many of these reactions, with channels such as charge transfer, hydride (H^-) abstraction, hydroxide (OH^-) abstraction, and insertion being common, although several other modes of reaction are observed. The overall reactivity of $S^+(^4S)$ is similar in many respects to that of $SO^+(^2\Pi_r)$, a closely related ion that is abundant in interstellar molecular clouds (ISC). The rate coefficients and product distributions for the reactions of $S^+(^4S)$ with the 20 molecules listed above are presented and discussed in terms of reaction mechanisms and product formation. Reactions of $S^+(^4S)$ and the corresponding reactions of $SO^+(^2\Pi_r)$ are compared, where possible, and discussed in terms of reaction mechanisms and significance to the chemistry of sulfur in ISC.

1. Introduction

Atomic ground-state $S^+(^4S)$ is expected to be an abundant interstellar ion[1−4] and an important precursor for the synthesis of sulfurated interstellar molecules in the gas phase.[2,5] Due to interest initially stimulated by the detection of the polycarbon sulfide radicals C_2S and C_3S in the Taurus Molecular Cloud (TMC-1) in 1987,[6,7] reactivity studies of this ion have focused particularly on its hydrocarbon chemistry.[1,8−10] Possible chemical pathways to form polycarbon sulfide radicals in interstellar clouds (ISC) have been considered,[1,8,9,11] especially via reactions involving $S^+(^4S)$ such as

$$S^+ + C_2H_2 \rightarrow HC_2S^+ + H \tag{1a}$$

$$HC_2S^+ + e \rightarrow C_2S + H \tag{1b}$$

Reaction 1a has been studied by experimental[1,10] and theoretical[9] methods, while the dissociative electron/ion recombination (1b) has yet to be investigated. Reactions of $S^+(^4S)$ with many small and mostly inorganic molecules of interstellar interest (e.g., H_2, HD, D_2, CO, O_2, N_2, NO, H_2O, H_2S, HCN, CO_2, OCS, SO_2, and NH_3) have also been studied.[12−16]

In contrast to the above situation, the reactivity of $S^+(^4S)$ with organic molecules other than hydrocarbons largely has been neglected. Reactions of S^+ with only a small number of nonhydrocarbon organic molecules (e.g., CH_2O, CH_3I, CH_3SH, and CH_3NH_2) have been studied.[12,13] Of these, only the reaction with CH_3NH_2 has been studied with a selected ion flow tube (SIFT).[14] The reaction with CH_2O is listed in a standard database of ion/molecule reactions,[12] from an unpublished ion cyclotron resonance (ICR) mass spectrometry study. The reactions with CH_3I[13,17] and CH_3SH[13,18] are reported from older work that did not employ fast flow techniques to spatially resolve the reaction region for determining the ion/molecule reaction kinetics and product distributions.

Because S^+ is overwhelmingly in its ^4S ground electronic state under the prevailing conditions in dense (i.e., $10^3−10^6$ cm^{-3} H_2)[19] ISC, it is unreactive with both H_2 and CO,[12,13] the major molecular constituents of ISC.[5,19,20] Thus, the reactivity of $S^+(^4S)$ with minority species in ISC is important for the interstellar chemistry of sulfur. One of the most abundant of such species is the hydroxyl radical, OH, with which $S^+(^4S)$ is expected to react to form SO^+:[21−23]

$$S^+ + OH \rightarrow SO^+ + H \tag{2}$$

Reaction 2 has not yet been studied in the laboratory. However, SO^+ is a ubiquitous interstellar ion[21] whose reactions with many organic molecules of interstellar interest have been investigated.[23] Hydrogenation of sulfur in ISC is thought to occur primarily by the protonation of neutral atomic $S(^3P)$:[2,5,24]

$$H_3{}^+ + S \rightarrow SH^+ + H_2 \tag{3}$$

$$HCO^+ + S \rightarrow SH^+ + CO \tag{4}$$

Reactions 3 and 4 have not yet been studied in the laboratory, although HCO^+,[25] and recently $H_3{}^+$,[25−27] have been detected in ISC, and exothermic proton transfers such as reactions 3 and 4 are generally efficient.[28,29] Another route to the hydrogenation of sulfur that has been considered is the reaction of S^+ with formaldehyde:[24]

$$S^+ + CH_2O \rightarrow H_2S^+ + CO \tag{5}$$

An unpublished ICR study of reaction 5 reported in a compilation of ion/molecule reactions[12] indicates a bimolecular rate coefficient of 6.7 × 10^{-10} cm^3 $molecule^{-1}$ s^{-1}, with a product

10.1021/jp992470p CCC: $19.00

distribution of $H_2S^+ + CO$ (50%); $HCO^+ + SH$ (50%).[12] Hydrogen sulfide (H_2S) has an observed abundance in dense ISC (such as TMC-1) that is much greater than predicted by interstellar chemical models;[2,30] thus, a careful consideration of possible routes to the formation of hydrogenated sulfur species is necessary. Another such species, the mercapto radical (SH), has not yet been observed in ISC,[25] although its oxygenated analogue (OH) is a well-known and abundant interstellar species and, indeed, was the first molecular interstellar species to be detected with a radio telescope.[31]

The identification of sulfurated species in ISC is difficult in comparison to the analogous oxygenated species, due to the lower cosmic abundance of sulfur than oxygen.[32,33] Also there is a greater difficulty in preparing the sulfurated species in the laboratory for accurate determination of their microwave rotational transitions, which is essential for their identification with radio telescopes.[30] Thus, only 14 of the ~114 species in a recent list of molecular species identified in ISC are S-bearing,[25] whereas 33 O-bearing molecules appear in the same list.[25] It has also become clear that, although sulfur is isovalent with oxygen, its chemistry in ISC is quite different from that of oxygen, and thus the relative abundances of S-bearing species and the analogous O-bearing species are not generally in proportion to the relative cosmic abundances of these elements.[30] Very little of the cosmic abundance of sulfur has so far been accounted for in dense ISC, either in the observed species in the gas phase[25] or locked up in icy grain mantles in the form of molecules such as OCS, SO_2, H_2CS, and H_2S.[34] Thus, the disposal of sulfur in dense ISC remains a current outstanding problem of interstellar chemistry. Reactivity studies of S-bearing ions are therefore necessary to improve interstellar chemical models. These then guide searches for new S-bearing interstellar species by predicting which of these are likely to be abundant.

The reactions of $S^+(^4S)$ with ~15 hydrocarbons have already been investigated.[1,8,10,12,13] The present work is intended to expand the data set for reactions of $S^+(^4S)$ to include small organic molecules containing oxygen and sulfur, which are observed or likely to be present in ISC.[25] We therefore have employed a SIFT to study the reactions of $S^+(^4S)$ with the following 20 molecules at 296 ± 4 K: CH_3OH, CH_3SH, C_2H_5OH, C_2H_5SH, CH_3OCH_3, CH_3SCH_3, CH_2O, CH_3CHO, C_2H_5CHO, $CH_3C(O)CH_3$, $C_2H_5C(O)CH_3$, HCO_2H, CH_3CO_2H, $C_2H_5CO_2H$, HCO_2CH_3, $HCO_2C_2H_5$, $CH_3CO_2CH_3$, $CH_3CO_2C_2H_5$, $C_2H_5CO_2CH_3$, and $C_2H_5CO_2C_2H_5$. Ten of these molecules have been detected in ISC (see Table 1),[25] and others among them are likely to be present. Several of the listed molecules, e.g., CH_3OH, CH_3OCH_3, HCO_2H, and HCO_2CH_3, are observed to have unusually high abundances in the so-called "Compact Ridge" region of the Kleinman–Low (KL) Nebula in the Orion Molecular Cloud.[35,36] In "hot cores" such as the ~100 K Compact Ridge, sulfur-bearing species also are predicted and observed to have high number densities;[37] thus, the reactions of $S^+(^4S)$ and other S-bearing ions such as SO^+ and S_2^+ with these relatively abundant organic molecules may be particularly important in such interstellar regions. Reactivity studies of SO^+ and S_2^+ with many of the molecules in the present study have been reported previously.[23,38,39]

2. Experimental Section

The SIFT technique has been described in detail elsewhere[40] and will only be outlined briefly here, with details relevant to the present experiments. Numerous ions (i.e., CS_2^+, S_2^+, CS^+, CS_2^{2+}, S^+, and C^+) were generated by impact of 70 eV electrons on carbon disulfide (CS_2) vapor in a low-pressure ion source. A series of electrostatic lenses guided the ion swarm into an upstream quadrupole mass filter, which selected S^+ with unit mass resolution from the other ions in the swarm. A second series of electrostatic lenses at the output side of the filter focused the S^+ ions through a 1.0 mm orifice in a molybdenum disk electrode, isolating the differentially pumped quadrupole housing from the flow tube. The swarm of S^+ entering the flow tube was captured into a fast flow of high-purity (BOC Ultra-Lab, 99.997%) helium introduced at a venturi-type inlet just downstream from the molybdenum disk. The helium had been further purified by passage through a liquid nitrogen-cooled molecular sieve trap prior to introduction into the flow tube. The helium pressure was established by regulating the throughput with a calibrated flowmeter (MKS) and evacuating the flow tube by the action of a Roots-type blower (Stokes) with a nominal pumping speed of 755 L s^{-1}. A laminar flow of the helium carrier gas was established within ~10 cm of the venturi inlet, with a plug flow velocity of ~8000 cm s^{-1} at a pressure of ~0.5 Torr. The S^+ ion swarm traveled at a higher group velocity of ~12 000 cm s^{-1}.[40] The center-of-mass translational energy of the ion swarm was thermalized to the laboratory temperature, 296 ± 4 K, by contact with the helium.

The S^+ ion swarm entering the flow tube contained a considerable population of ^2P and ^2D metastable excited S^+, as well as ground-state $S^+(^4S)$ (see Figure 1a). The metastable states of S^+ are known to react with H_2 to form SH^+,[1] as shown in Figure 1b. Ground-state $S^+(^4S)$ is unreactive with H_2.[1] To monitor the presence of $S^+(^2P,^2D)$ metastables, a flow of H_2 sufficient to ensure complete conversion of $S^+(^2P,^2D)$ into SH^+ was maintained. High-purity N_2 (BOC, 99.999%) was added as a quenchant at a reagent inlet near the helium venturi inlet, ~80 cm upstream from the point of H_2 addition. The end point for titration, or total quenching, of the metastable $S^+(^2P,^2D)$ by N_2 was noted (see Figure 1c). The H_2 flow was then removed, and the reactions in the present study were investigated with a

TABLE 1: Experimentally Determined Bimolecular Rate Coefficients, $k_{exp}^{(2)}$, and Reaction Efficiencies, $k_{exp}^{(2)}/k_{th}^{(2)}$, for the Reactions of $S^+(^4S)$ with the Indicated Molecules at 296 ± 4 K

formula	μ (D)[a]	detected in ISC[b](*)	$10^9 k_{exp}^{(2)}$ (cm^3 molecule^{-1} s^{-1})	efficiency ($k_{exp}^{(2)}/k_{th}^{(2)}$)[c]
CH_3OH	1.70	*	1.7	0.75
CH_3SH	1.52	*	2.1	1.01
C_2H_5OH	1.69	*	2.3	1.01
C_2H_5SH	1.60		2.1	0.94
CH_3OCH_3	1.28	*	1.8	0.95
CH_3SCH_3	1.55		2.2	1.01
H_2CO	2.33	*	1.9	0.67
CH_3CHO	2.75	*	3.3	1.02
C_2H_5CHO	2.52		3.0	1.01
$CH_3C(O)CH_3$	2.88	*	3.3	1.02
$C_2H_5C(O)CH_3$	2.78		3.2	0.99
HCO_2H	1.41	*	1.7	0.93
CH_3CO_2H	1.70	*	2.0	0.90
$C_2H_5CO_2H$	1.75		2.2	0.97
HCO_2CH_3	1.77	*	1.8	0.81
$HCO_2C_2H_5$	1.90		1.9	0.77
$CH_3CO_2CH_3$	1.72		1.7	0.79
$CH_3CO_2C_2H_5$	1.78		1.8	0.75
$C_2H_5CO_2CH_3$	1.70		1.7	0.74
$C_2H_5CO_2C_2H_5$	1.75		1.9	0.80

[a] Electric dipole moments, μ, are taken from standard compilations.[49,50] [b] The symbol * indicates that the molecule has been detected in at least one interstellar molecular cloud (ISC). [c] The theoretical capture rate coefficient, $k_{th}^{(2)}$, was determined using the model of Su and Chesnavich.[48] Electric dipole moments and electric dipole polarizabilities necessary to calculate $k_{th}^{(2)}$ were obtained from standard compilations.[49,50]

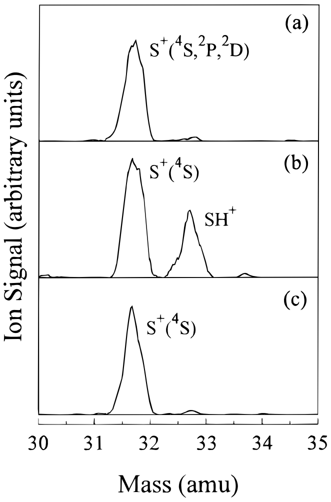

Figure 1. Demonstration of the quenching of metastable $S^+(^2P,^2D)$ by N_2. (a) S^+ generated from CS_2 (see text) was injected into the fast flow of He carrier gas; the downstream quadrupole mass spectrometer resolves a peak at $m/z = 32$ due to a mixture of S^+ ground-state and metastable ions. The small peak at $m/z = 33$ is due to incomplete elimination of the $^{33}S^+$ isotope in the injection mass filter. (b) H_2 was added to the flow to convert the metastable $S^+(^2P,^2D)$ entirely to SH^+ ($m/z = 33$) via ion/molecule reactions; the ground-state $S^+(^4S)$ does not react with H_2 under thermal conditions (see text). (c) N_2 quenchant was added in excess far upstream from the region of H_2 addition; note that $S^+(^2P,^2D)$ have been entirely converted to $S^+(^4S)$, and therefore at $m/z = 33$ only the residual signal due to $^{33}S^+(^4S)$ again is observed.

quenching flow of N_2 ~5 times the flow at the titration end point, to ensure complete conversion of $S^+(^2P,^2D)$ into $S^+(^4S)$ well upstream from the reaction region.

Neutral reactants were introduced into the flow tube at fixed ring-type[40] inlet ports, thereby establishing characteristic reaction lengths, and hence, reaction times. Neutral reactant flows were determined by measuring the input pressure and the pressure drop across a calibrated capillary tube in the reactant flow line, which required a knowledge of the gas or vapor viscosity of each neutral reagent. These were either obtained from a compilation[41] or were determined experimentally by measuring the time dependence of the pressure drop in a calibrated volume filled with the reagent vapor as it was evacuated through the calibrated capillary tube. Reagents were obtained from commercial sources with the following purities: CS_2 (99.99 wt %), CH_3OH (99.9+ wt %), CH_3SH (99.5+ %), C_2H_5OH (200.0 proof), C_2H_5SH (99.6 wt %), CH_3OCH_3 (99.87 mol %), CH_3SCH_3 (99.3 wt %), CH_2O (paraformaldehyde, 95 wt %), CH_3CHO (99.4 wt %), C_2H_5CHO (99.7 wt %), $CH_3C(O)CH_3$ (99.90 wt %), $C_2H_5C(O)CH_3$ (99.5+ wt %), HCO_2H (99.4 wt %), CH_3CO_2H (99.99+ wt %), $C_2H_5CO_2H$ (99.9 wt %), HCO_2CH_3 (99.35 wt %), $HCO_2C_2H_5$ (98.6 wt %), $CH_3CO_2CH_3$ (99.98 wt %), $CH_3CO_2C_2H_5$ (99.98 wt %), $C_2H_5CO_2CH_3$ (99.94 wt %), $C_2H_5CO_2C_2H_5$ (99.4 wt %). Reagent gases (i.e., CH_3SH and CH_3OCH_3) were used without further purification, and reagent liquids were purified by several freeze−pump−thaw cycles before use. Formaldehyde was introduced into the flow line by sublimation of paraformaldehyde at ~110 °C. The carboxylic acids (i.e., HCO_2H, CH_3CO_2H, and $C_2H_5CO_2H$) were prepared in dilute (0.5%−1.5%) manometric mixtures with pure (99.997%) helium, which had been further purified by passage through a liquid nitrogen-cooled molecular sieve trap. Corrections were made for the shift in the monomer/dimer equilibria of the carboxylic acids upon dilution (the magnitudes of these corrections have been discussed earlier[38]), using available literature data.[42,43] It was justifiably assumed that, at the small mixing ratios, the viscosities of the dilute carboxylic acid mixtures with helium were equal to the viscosity of helium within a negligible error.

The $S^+(^4S)$ and product ions were sampled downstream through a 0.3 mm orifice in a molybdenum disk electrode mounted in a nose cone separating the flow tube at ~0.5 Torr from the differentially pumped downstream quadrupole mass spectrometer housing at $\sim 10^{-5}$ Torr. These ions were directed by a series of electrostatic lenses into the quadrupole mass spectrometer (Extrel C-60) and were mass-selected with unit mass resolution. The ions emerging from the mass spectrometer were detected by an on-axis channel electron multiplier (Detech), whose signals were amplified and then passed to a gated pulse counter (Stanford Research Systems SR400). Sweeping of the mass spectrometer and processing of the ion signals were handled on-line by in-house software with a desktop computer. Reaction rate coefficients and product distributions were determined as described previously.[44,45] Rate coefficients are estimated to be accurate to ±20% for permanent gases and ±30% for "sticky" vapors and mixtures, although reproducibility was generally better than ±10% in this and our previous studies[23,38,39] (for example, the 95% sample confidence interval from five determinations of the rate coefficient for the $S^+(^4S) + C_2H_5CO_2CH_3$ reaction in this study is $(1.67 \pm 0.16) \times 10^{-9}$ cm^3 $molecule^{-1}$ s^{-1}). Product distributions are considered to be accurate to ±0.05. Where necessary, corrections for mass discrimination in the detection system were made as described previously;[39] such corrections were not generally necessary in the present study, since most of the primary ion products appeared where there was no relative mass discrimination. Corrections were also made to the primary ion product distributions for small contributions due to the isotopes of neighboring ion products, particularly the ^{13}C and the ^{34}S isotopes,[46] where necessary. Note that the estimated ±0.05 accuracy in the product distributions places some uncertainty on whether those fractional product channels <0.05 of the product spectra are actually present. However, because of the high purities of most of the reagents and of the carrier and quench gases (see above), and because $S^+(^4S)$ can be cleanly established as the only primary reactant ion in the flow tube, in most cases there is no a priori reason to omit these minority product channels from the product distributions. Potential products contributing <0.01 to the product spectra were omitted from the product distributions since they could be produced from impurities in the reagents.

3. Results and Discussion

Figure 2a illustrates a sample of the data collected in the present study. The figure shows a log-linear rate-decay plot for the reaction of $S^+(^4S)$ with CH_3OH. The decay of $S^+(^4S)$ as a function of CH_3OH flow demonstrates excellent linearity over 3 orders of magnitude (correlation to the fit line = 0.9997). Such linearity in the decay and the absence of a charge-transfer product channel with CH_3OH (which has an ionization energy (IE) of 10.84 eV, larger than the recombination energy (RE) of 10.36 eV for $S^+(^4S)$,[46] but smaller than those of $S^+(^2D,^2P)$ (>12.20 eV)[47]) indicates the absence of any metastable $S^+(^2P,^2D)$ in the reaction region, as shown above (see Experimental Section). Figure 2b illustrates the primary ion product distribution for the same reaction. Extrapolation to zero CH_3OH flow on the plot yields the nascent ion product distribution for the primary reaction.

Data such as those illustrated in Figure 2a have been used to determine the bimolecular rate coefficients, $k_{exp}^{(2)}$, for the reactions of $S^+(^4S)$ with the 20 molecules in the present study.

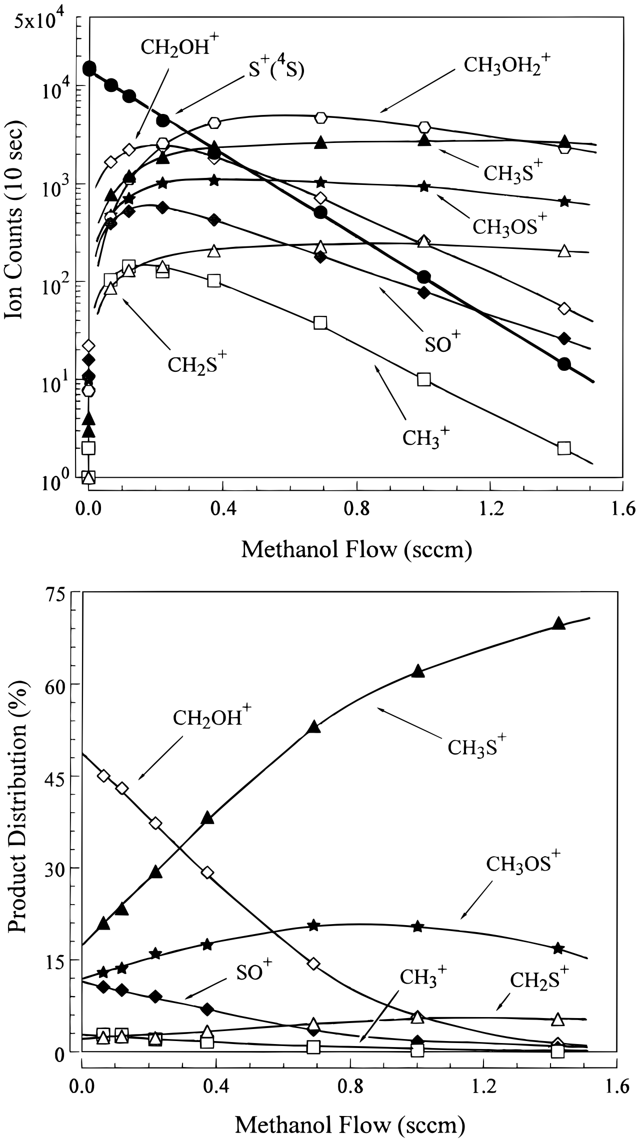

Figure 2. (a) Variation of $S^+(^4S)$ and ion product signals with CH_3OH flow and (b) percentages of the ion products as a function of CH_3OH flow. The decay of $S^+(^4S)$ in (a) shows excellent linearity over 3 orders of magnitude. Because of the numerous product channels evident in this reaction, the two most minor ion products are omitted from both (a) and (b) for clarity (see Table 2). Similarly, all secondary and higher order products are omitted except for the dominant secondary product, $CH_3OH_2^+$, in (a). Ion products are indicated in their expected empirical and structural forms, as explained in the text. Nascent ion product distributions and binary rate coefficients deduced from these and other data are presented in Table 2.

These data are presented in Table 1, along with the corresponding reaction efficiencies expressed as ratios between $k_{exp}^{(2)}$ and the theoretical capture rate coefficients at 296 K, $k_{th}^{(2)}$, calculated from the parametrized variational transition state theory of Su and Chesnavich[48] (electric dipole moments and electric dipole polarizabilities necessary for these calculations were obtained from standard reference compilations[49,50]). At the experimental temperatures, $k_{exp}^{(2)} \geq {}^2/_3 k_{th}^{(2)}$ for all of the reactions studied (see Table 1), and thus, all proceed with high efficiency. Note that all 20 neutral reactants have substantial electric dipole moments (see Table 1), and therefore the rate coefficients, assuming similar reaction efficiencies, are expected to be larger at the lower temperatures prevalent in ISC (∼20 K for cold, dense ISC such as TMC-1[19] and ∼100−200 K for "hot" clumps such as the Compact Ridge in the Orion KL Nebula[36]) due to improved charge/dipole locking.[51,52] The reactions of $S^+(^4S)$ with hydrocarbons are also rapid, as noted by Smith et al.[1] Thus, the high spin-multiplicity of S^+ in its quartet ground state does not generally hinder its reactivity, implying either that products are formed in low-lying high-spin electronic states or that spin flipping in the reactions of $S^+(^4S)$ is facile.[1] No evidence for termolecular reactions (three-body collisional association) of $S^+(^4S)$ with any of the neutral molecules was observed in the present study or that of Smith et al.

3.1. Product Distributions for the $S^+(^4S)$ Reactions. Product distribution plots such as Figure 2b have been used to determine the nascent primary ion product distributions for the reactions of $S^+(^4S)$ shown in Table 2. Primary ion products are indicated by their mass-to-charge ratios (*m/z*), which are unequivocal, and also by their expected empirical (i.e., atomic constituency) and structural identities, where possible; explanations for these choices are presented below. Charge (electron) transfer to the neutral molecule, M, is signified in the ion product column simply by M^+ for compactness. The RE of 10.36 eV for $S^+(^4S)$ (see above) lies in the midst of the range of IE's of the 20 neutral reactants in the present study (see Table 2) and also of the 14 hydrocarbons in the study of Smith et al.[1] Thus, the quantity $RE(S^+(^4S)) - IE(M) \leq 40$ kcal mol^{-1}, which is substantially less than the strength of any of the bonds occurring in these 34 molecules. All simple charge transfer (i.e., electron jump) reactions of $S^+(^4S)$ with these molecules are therefore nondissociative, and thus the product channel in which M^+ appears represents the total contribution of simple charge transfer to the product spectrum. A plot of the efficiency of charge transfer (defined as the product of the branching fraction, *f*, of the M^+ channel and the overall reaction efficiency, $k_{exp}^{(2)}/k_{th}^{(2)}$; see Tables 1 and 2) as a function of $RE(S^+(^4S)) - IE(M)$ for the reactions of $S^+(^4S)$ with the 34 molecules is shown in Figure 3. This demonstrates a very strong correlation of simple charge transfer efficiency with charge-transfer exothermicity. Such behavior is to be expected for the reactions of atomic ions with polyatomic molecules (which have a high density of rovibronic states), as has been discussed in more detail in a recent review.[28]

Apart from charge transfer, numerous other product channels occur in the reactions of $S^+(^4S)$ with the molecules in the present study (see Table 2). For the purpose of discussion, these molecules are divided into three functional groupings (with R, R′ = H, CH_3, or C_2H_5): (a) R−O−R′ and R−S−R′ (alcohols, thiols, ethers, and sulfides); (b) R−C(O)-R′ (aldehydes and ketones); (c) R−C(O)-OR′ (carboxylic acids and esters). Some variations in product channeling among these different groupings are apparent and are discussed below. Often branching into many significant product channels is observed in these reactions, with branching fractions governed more by product stability than by the particular reaction mechanisms. Note that in the discussions which follow, a particular reaction channel is often referred to by its alphanumeric label, as given in Table 2. Reaction enthalpies are calculated from data available in refs 53 and 54 (except where otherwise specified) in order to determine or at least to discuss the energetically allowed products.

3.1a. Reactions of $S^+(^4S)$ with R−O−R′ and R−S−R′. Charge transfer dominates the reactions of $S^+(^4S)$ with the sulfur-bearing molecules (CH_3SH, C_2H_5SH, and CH_3SCH_3), which is expected from the relatively large values of $RE(S^+(^4S)) - IE(M)$ for these reactions (see Table 2). The remaining significant product channels with the thiols (CH_3SH and C_2H_5SH) are analogous to those observed with the corresponding alcohols. Hydride (H^-) transfer is dominant with CH_3OH and CH_3OCH_3, whereas hydroxide (OH^-) transfer is dominant with C_2H_5OH. Hydroxide

TABLE 2: Fractional Product Distributions, *f*, of Ion Products Detected at Mass-to-Charge Ratio *m*/*z*, and the Proposed Neutral Products for the Reactions of $S^+(^4S)$ with the Indicated Organic Molecules, M, at 296 ± 4 K[a]

reactant (M)	IE[b] (eV)	reacn channel	*f*	*m*/*z*	ion prod[c]	neutral prod[d]
		R−O−R′ and R−S−R′				
CH_3OH, methanol	10.84	1. a	0.50	31	CH_2OH^+	HS
		b	0.17	47	CH_3S^+	HO
		c	0.12	63	CH_3SO^+	H
		d	0.12	48	SO^+	CH_4
		e	0.03	15	CH_3^+	HSO
		f	0.02	46	CH_2S^+	H_2O
		g	0.02	34	H_2S^+	CH_2O
		h	0.02	49	HSO^+	CH_3
CH_3SH, methanethiol	9.44	2. a	0.85	48	M^+	S
		b	0.15	47	CH_2SH^+	HS
C_2H_5OH, ethanol	10.48	3. a	0.53	29	$C_2H_5^+$	HSO
		b	0.22	45	$C_2H_5O^+$	HS
		c	0.13	50	$HSOH^+$	C_2H_4
		d	0.07	63	CH_3SO^+	CH_3
		e	0.05	31	CH_2OH^+	CH_3S
C_2H_5SH, ethanediol	9.31	4. a	0.75	62	M^+	S
		b	0.15	29	$C_2H_5^+$	HS_2
		c	0.03	61	$C_2H_5S^+$	HS
		d	0.02	66	$HSSH^+$	C_2H_4
		e	0.02	27	$C_2H_3^+$	$HS + H_2S$
		f	0.02	47	CH_2SH^+	CH_3S
		g	0.01	28	$C_2H_4^+$	HS + HS
CH_3OCH_3, dimethyl ether	10.03	5. a	0.40	45	$CH_3OCH_2^+$	HS
		b	0.35	46	M^+	S
		c	0.20	63	CH_3SO^+	CH_3
		d	0.03	29	$C_2H_5^+$	HSO
		e	0.02	15	CH_3^+	CH_3SO
CH_3SCH_3, dimethyl sulfide	8.69	6. a	0.92	62	M^+	S
		b	0.03	47	CH_3S^+	CH_3S
		c	0.02	79	$CH_3S_2^+$	CH_3
		d	0.02	61	$CH_3SCH_2^+$	HS
		e	0.01	46	CH_2S^+	CH_3SH
		R−C(O)−R′				
CH_2O, formaldehyde	10.88	7. a	0.65	29	HCO^+	HS
		b	0.35	34	H_2S^+	CO
CH_3CHO, acetaldehyde	10.23	8. a	0.30	43	CH_3CO^+	HS
		b	~0.20	48	CH_3SH^+	CO
		c	~0.15	48	SO^+	C_2H_4
		d	0.08	50	$HSOH^+$	C_2H_2
		e	0.08	44	M^+	S
		f	0.07	47	CH_3S^+	HCO
		g	0.05	28	$C_2H_4^+$	SO
		h	0.03	29	HCO^+	CH_3S
		i	0.02	59	CH_3CS^+	HO
		j	0.02	46	CH_2S^+	CH_2O
C_2H_5CHO, propionaldehyde	9.96	9. a	0.40	41	$C_3H_5^+$	HSO
		b	0.17	42	$C_3H_6^+$	SO
		c	0.15	58	M^+	S
		d	0.12	29	$C_2H_5^+$	HCOS
		e	0.10	57	$C_2H_5CO^+$	HS
		f	0.03	28	C_2H_4+	HS + HCO
		g	0.02	73	$C_3H_5S^+$	HO
		h	0.01	61	$C_2H_5S^+$	HCO
$CH_3C(O)CH_3$, acetone	9.70	10. a	0.65	41	$C_3H_5^+$	HSO
		b	0.15	43	CH_3CO^+	CH_3S
		c	0.14	58	M^+	S
		d	0.04	42	$C_3H_6^+$	SO
		e	0.02	29	$C_2H_5^+$	HCOS
$C_2H_5C(O)CH_3$, 2-butanone	9.52	11. a	0.36	72	M^+	S
		b	0.23	43	CH_3CO^+	C_2H_5S
		c	0.17	55	$C_4H_7^+$	HSO
		d	0.12	57	$C_2H_5CO^+$	CH_3S
		e	0.07	56	$C_4H_8^+$	SO
		f	0.03	29	$C_2H_5^+$	$CH_3S + CO$
		g	0.02	41	$C_3H_5^+$	CH_3SO
		R−C(O)−OR′				
HCO_2H, formic acid	11.33	12. a	0.85	50	$HSOH^+$	CO
		b	0.15	29	HCO^+	HSO
CH_3CO_2H, acetic acid	10.65	13. a	1.00	43	CH_3CO^+	HSO
$C_2H_5CO_2H$, propionic acid	10.44	14. a	0.50	57	$C_2H_5CO^+$	HSO
		b	0.43	29	C_2H_5+	HSO + CO
		c	0.02	28	C_2H_4+	$H_2S + CO_2$
		d	0.02	73	$(M - H)^+$	HS
		e	0.02	60	$C_2H_4S^+$	HCOOH
		f	0.01	59	$C_2H_3O_2^+$	CH_3S
HCO_2CH_3, methyl formate	10.84	15. a	0.30	31	CH_2OH^+	HCOS
		b	0.20	64	CH_3SOH^+	CO
		c	0.13	47	CH_3S^+	HCO_2
		d	0.10	48	SO^+	$CH_4 + CO$
		e	0.09	34	H_2S^+	$CH_2O + CO$
		f	0.08	62	CH_2SO^+	CH_2O
		g	0.05	63	CH_3SO^+	HCO
		h	0.03	29	HCO^+	$HS + CH_2O$
		i	0.02	46	CH_2S^+	HCOOH
$HCO_2C_2H_5$, ethyl formate	10.61	16. a	0.45	50	$HSOH^+$	$C_2H_4 + CO$
		b	0.35	29	$C_2H_5^+$	HSO + CO
		c	0.08	63	CH_3SO^+	CH_3CO
		d	0.06	45	$C_2H_5O^+$	HCOS
		e	0.02	59	$CH_3CO_2^+$	CH_3S
		f	0.02	47	CH_3S^+	$CH_3 + CO_2$
		g	0.01	60	$C_2H_4S^+$	HCOOH
		h	0.01	61	$C_2H_5S^+$	HCO_2
$CH_3CO_2CH_3$, methyl acetate	10.25	17. a	0.70	43	CH_3CO^+	CH_3SO
		b	0.15	57	$C_3H_5O^+$	HSO
		c	0.08	59	CH_3OCO^+	CH_3S
		d	0.03	47	CH_3S^+	$CH_3 + CO_2$
		e	0.02	46	CH_2S^+	CH_3COOH
		f	0.01	56	$C_3H_6O^+$	SO
		g	0.01	74	M^+	S
$CH_3CO_2C_2H_5$, ethyl acetate	10.01	18. a	0.88	43	CH_3CO^+	C_2H_5SO
		b	0.05	88	M^+	S
		c	0.04	29	$C_2H_5^+$	$CH_3SO + CO$
		d	0.01	60	$C_2H_4S^+$	CH_3COOH
		e	0.01	59	$C_2H_3O_2^+$	$HS + C_2H_4$
		f	0.01	61	$C_2H_5S^+$	$CH_3 + CO_2$
$C_2H_5CO_2CH_3$, methyl propionate	10.15	19. a	0.30	57	$C_2H_5CO^+$	CH_3SO
		b	0.17	61	$C_2H_5S^+$	$CH_3 + CO_2$
		c	0.10	71	$C_4H_7O^+$	HSO
		d	0.10	28	$C_2H_4^+$	$H_2S + CO + CH_2O$
		e	0.10	60	$C_2H_4S^+$	$HCOOCH_3$
		f	0.07	59	CH_3OCO^+	$HS + C_2H_4$
		g	0.05	88	M^+	S
		h	0.03	72	$C_4H_8O^+$	SO
		i	0.02	29	$C_2H_5^+$	$CH_3SO + CO$
		j	0.02	87	$(M - H)^+$	HS
		k	0.02	55	$C_2H_3CO^+$	$H_2S + CH_3O$
		l	0.01	73	$C_3H_5O_2^+$	CH_3S
		m	0.01	74	$C_3H_6O_2^+$	CH_2S
$C_2H_5CO_2C_2H_5$, ethyl propionate	10.00	20. a	0.75	57	$C_2H_5CO^+$	C_2H_5SO
		b	0.10	29	$C_2H_5^+$	$HS + C_2H_4 + CO_2$
		c	0.09	102	M^+	S
		d	0.03	60	$C_2H_4S^+$	C_2H_5COOH
		e	0.01	61	$C_2H_5S^+$	$C_2H_5 + CO_2$
		f	0.01	28	$C_2H_4^+$	$H_2S + C_2H_4 + CO_2$
		g	0.01	59	$C_2H_3O_2^+$	$CH_3S + C_2H_4$

[a] For comparison, the recombination energy (RE) of $S^+(^4S)$ is 10.36 eV.[46,53] [b] First ionization energies (IE) of the indicated neutral molecules are taken from ref 53. [c] See the text for further discussions on the identities of these ion products. Charge transfer to the molecule, M, is indicated in the ion product column by M^+ for compactness; in two cases, hydride (H^-) abstraction is similarly indicated by $(M - H)^+$. [d] Neutral products are suggested only, since they are not directly observed. See the text for details.

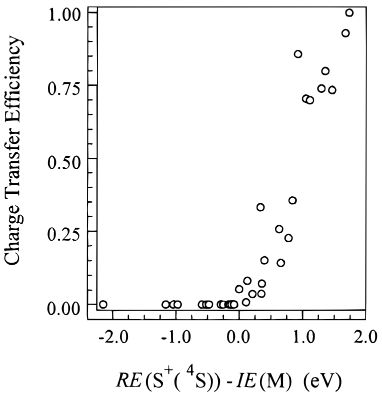

Figure 3. Efficiency of simple charge (electron) transfer (defined in the text) versus $RE(S^+(^4S)) - IE(M)$, where $RE(S^+(^4S))$ is the recombination energy of $S^+(^4S)$ and the IE(M) are the ionization energies of the 34 neutral molecules in the present study and that of Smith et al.[1] Note that the overall efficiencies of the reactions are almost universally high, and therefore the plot illustrates the competitiveness of the charge-transfer channel with other binary reaction channels; ternary channels are not observed. Little (<1%) or no endothermic charge transfer is observed in these fast reactions. Updated product distributions have been used to construct the present plot from that in ref 28, and the ordinate ("charge-transfer efficiency") is defined somewhat differently.

transfer frequently occurs as a reaction channel, leading to the formation of either the thioperoxy radical, HSO, or its structural isomer, HOS. In a definitive high-level ab initio study, Xantheas and Dunning[55] have determined that $\Delta H_f^{\circ 298}(HSO) = -6.1 \pm 1.3$ kcal mol^{-1} and $\Delta H_f^{\circ 298}(HSO) = -0.7 \pm 1.3$ kcal mol^{-1}, with an isomerization barrier of 46.3 kcal mol^{-1} and a dissociation energy to $H(^2S) + SO(^3\Sigma^-)$ of 56.2 kcal mol^{-1} above HSO.[55] Thus, the two isomers only lie 5.4 kcal mol^{-1} apart in energy, with a rather high barrier to isomerization, and formation of either HSO or HOS is energetically possible in most of the OH^- abstraction channels in these reactions (in a more recent study at a higher level of theory,[56] HOS was found to lie 7.4 kcal mol^{-1} above HSO). An exception is channel 1e in the reaction with CH_3OH, which is only 1.8 kcal mol^{-1} exothermic to form HSO but is 5.6 kcal mol^{-1} endothermic to form HOS.[53,56] An endothermicity of this magnitude would result in a reaction efficiency of $\sim 10^{-4}$ for HOS production and thus this would be unlikely to compete with HSO production. Although channel 1e is only 3% of the product distribution, it is highly likely to be a true product channel, because $m/z = 15$ is unequivocally CH_3^+ since there is not enough energy available to form NH^+ (which is the only conceivable alternative), and no ion products appear below $m/z = 15$, making interference from isotopic contributions impossible. Channel 1e is the only ion product channel in the present study for which the isomeric form (HSO vs HOS) of the OH^- abstraction product can be deduced from energetics, although mechanistic arguments can be used in other cases (see below).

In the reaction with CH_3OH, other product identifications can also be made on the basis of energetics. In channel 1a, for example, production of the hydroxymethyl cation, CH_2OH^+ (exothermic by 52.1 kcal mol^{-1})[53] must occur instead of the methoxy cation, CH_3O^+ (endothermic by 27.5 kcal mol^{-1}).[53,57] This result is interesting in that CH_3O^+ is a triplet in its ground state and CH_2OH^+ is a singlet. Thus, the reaction to form CH_3O^+ and the doublet SH is spin-allowed, but energetically forbidden; the opposite is true with formation of CH_2OH^+. That channel 1a is an important channel in an efficient reaction implies that spin conservation is not important or that the CH_2OH^+ can be formed in a triplet excited state. In channel 1c, the isomeric form of the ion is not CH_3OS^+, which is energetically forbidden.[53,58,59] However, several other isomeric forms, e.g., CH_2SOH^+, CH_2OSH^+, CH_3SO^+, etc., are possible,[59] and the product is written generically as CH_3SO^+, with no intention to imply structure (the CH_3SO^+ ion product in channel 5c also has an unspecified structure). The products at $m/z = 48$ (channel 1d) must be $SO^+ + CH_4$, since formation of $CH_3SH^+ + O$ is endothermic by 15.1 kcal mol^{-1}.[53] Finally, it should be noted that channel 1h, forming $HSO^+ + CH_3$, seems somewhat improbable because of isotope contamination from the products at $m/z = 47$ (CH_3S^+) and $m/z = 48$ (SO^+). However, IE(HSO) = 9.92 eV,[60] which is quite close to IE(CH_3) = 9.84 eV.[53] Thus, one would expect CH_3 and HSO to be in close competition for the charge in the decomposition of the activated complex (CH_4SO^+), according to Stevenson's Rule.[61] That the $CH_3^+ +$ HSO channel is observed, although small, is added evidence for the existence of an $HSO^+ + CH_3$ channel.

The reaction with CH_3SH proceeds with a somewhat larger rate coefficient than reported previously in a much earlier study (see Table 1; the former value is $k_{exp}^{(2)} = 1.5 \times 10^{-9}$ cm^3 molecule^{-1} s^{-1}),[13,18] although the values overlap to within experimental error. Additionally, a 15% H^- abstraction channel (channel 2b) forming CH_3S^+ or CH_2SH^+ occurs, which was not reported previously. The isomeric form of CH_3S^+ is not constrained by reaction energetics,[53,62] so a mixture of the isomers arising from abstraction of the S-bonded hydrogen and one of the C-bonded hydrogens is possible. Similarly, the thiomethoxy (CH_3S) and the mercaptomethyl (CH_2SH) radicals are both energetically possible,[53] where CH_3S is inferred as a neutral product (see, e.g., channel 3e). Because IE(CH_3S) is higher than IE(CH_2OH), whereas IE(CH_2SH) is comparable,[53] it is thought that channel 3e forms CH_3S rather than CH_2SH as a neutral product, again by Stevenson's Rule.[61] In the reaction with CH_3OCH_3 (channel 5b), although most of the ion product at $m/z = 46$ is expected to be M^+ due to charge transfer, some admixture of CH_2S^+ is also possible. However, inspection of the reactions in Table 2 shows that CH_2S^+ is an infrequent, and always a very minor, ion product.

Note that in three cases (i.e., channels 1(a,g), 3(a,c), and 4(b,d)), competition for a proton between the leaving fragments in the activated complex occurs. Such behavior has been noted previously in the reactions of SO^+ [23] and S_2^+ [38,39] and occurs elsewhere in the present reaction set with $S^+(^4S)$ (see discussions below and Table 2). The leaving fragment with the higher proton affinity (PA) generally appears in the dominant channel, although barriers to internal proton transfer can skew the distribution, as is evident in the reaction with CH_2O (see Table 2, channels 7a,b), where SH has a higher PA than CO.[63,64]

3.1b. Reactions of $S^+(^4S)$ with R−C(O)−R′. The reaction of $S^+(^4S)$ with CH_2O has a rate coefficient, $k_{exp}^{(2)} = 1.9 \times 10^{-9}$ cm^3 molecule^{-1} s^{-1}, about 3 times larger than the previously reported value of 6.7×10^{-10} cm^3 molecule^{-1} s^{-1},[12] and with a slightly different distribution of the two products[12] (see Tables 1 and 2 and the Introduction). The previous results were reported in a compilation from an unpublished ICR study.[12] The magnitude of the discrepancy in the measured rate coefficient is likely due to difficulties in handling the CH_2O, which must be generated from paraformaldehyde by sublimation under heating and which can irreversibly condense to form a trimer under excessive heat. Note that such an error in handling would reduce the throughput of CH_2O monomer, likely resulting in a smaller rate of decay in the parent ion, and hence, a smaller measured rate coefficient. The reaction of $S^+(^4S)$ with CH_2O can best be described as an initial H^- abstraction to form the mercapto radical, HS, followed by competition for a proton between HS and CO.

The other reactions of $S^+(^4S)$ with aldehydes and ketones have not been reported previously. Extensive product branching is observed in these reactions, especially with acetaldehyde. Two channels giving an ion product at $m/z = 48$ are energetically possible in this reaction, viz., $CH_3SH^+ + CO$ (channel 8b) and $SO^+ + C_2H_4$ (channel 8c). Moreover, the complementary channels are both observed: channels 8h and 8b, implying intramolecular competition for a proton as discussed above, and channels 8g and 8c, implying competition for the charge between SO (IE = 10.29 eV)[53] and C_2H_4 (IE = 10.51 eV)[53] according to Stevenson's Rule.[61] Abstraction of the oxygen atom is evident in the reaction with C_2H_5CHO, forming $C_3H_6^+ +$ SO (IE = 9.73 eV for propene),[53] and also in the reactions with the two ketones, acetone and 2-butanone, and to a smaller extent in some of the reactions with the esters (see Table 2).

In the reaction with CH_3CHO, it was observed that the contribution of $m/z = 48$ to the nascent primary product distribution is 0.35 (see Table 2). From our former study[23] it is known that SO^+ reacts rapidly with CH_3CHO entirely to form CH_3CO^+. On the other hand, CH_3SH^+ is expected to react with CH_3CHO principally by proton transfer to form CH_3CHOH^+, since the proton affinity (PA) of CH_2SH is 175.4 kcal mol^{-1}, which is substantially lower than PA(CH_3CHO) = 183.7 kcal mol^{-1}.[29,63] Similarly, the other primary products $HSOH^+$, CH_3CHO^+, CH_3S^+, $C_2H_4^+$, and HCO^+ should also react with CH_3CHO principally by proton transfer, due to the lower PA's of HSO,[28,56] CH_3CO, CH_2S, C_2H_3, and CO.[63] The product CH_3CS^+ does not react further, and both CH_3CS^+ and CH_2S^+ have very small branching fractions. Thus, the secondary reaction of SO^+ with CH_3CHO is the only one that significantly contributes additional ion signal to the observed CH_3CO^+. The nascent branching fraction of the CH_3CO^+ channel is 0.30, and the peak CH_3CO^+ signal (which does not appreciably react further) is ~0.45 of the initial $S^+(^4S)$ signal. Since there is no significant relative mass discrimination between $S^+(^4S)$ and CH_3CO^+ (see Experimental Section), 0.15 of this peak CH_3CO^+ signal must arise from the SO^+ reaction. We therefore infer that, of the 0.35 contribution at $m/z = 48$, the branching fraction contributions from the SO^+ and the CH_3SH^+ channels are ~0.15 and ~0.20, respectively, as indicated in Table 2.

With all of the aldehydes and ketones except CH_2O, OH^- abstraction is observed, and indeed, is the dominant reaction channel with C_2H_5CHO and its structural isomer, $CH_3C(O)CH_3$. Because there is initially no O−H connectivity in any of these molecules, it is likely that HSO rather than HOS is formed as the neutral fragment; reaction enthalpy in all cases is insufficient to drive the HSO $\leftrightarrow$ SOH isomerization.[53-55] With CH_3CHO, the protonated form, $HSOH^+$, appears, as it does in several other reactions (see Table 2).

The product distributions in these reactions with aldehydes and ketones primarily reflect competition among a series of channels including the OH^- abstraction, O^- abstraction, α-cleavage (to form the acetyl or propionyl cation, CH_3CO^+ or $C_2H_5CO^+$, respectively) and charge-transfer channels. Channels forming CH_3CO^+ have larger branching fractions compared to those producing $C_2H_5CO^+$ (cf. channels 8a, 9e, 10b, 11b,d). Additionally, formation of $C_2H_5^+$ in the reactions with propionaldehyde (channel 9d) and with acetone (channel 10e) occurs, implying the formation of a neutral fragment or fragments containing [H, C, O, S]. If the fragment is formed with the connectivity H−S−C−O, the excess reaction energy is likely to induce dissociation to HS + CO, whereas the isomer H−C−O−S is rather stable against isomerization or dissociation to H + OCS.[65] The H−C−O−S intermediate is more likely, since it implies an initial interaction between the positively charged sulfur atom and the electron-rich carbonyl oxygen of the neutral molecule. A few other minor product channels also occur with these reactions (see Table 2).

3.1c. Reactions of $S^+(^4S)$ with R−C(O)−OR′. The reactions of $S^+(^4S)$ with carboxylic acids and esters are generally dominated by cleavage, ostensibly at the acyl−oxygen bond, to form the RCO^+ ion and a neutral fragment or fragments. With HCO_2H and CH_3CO_2H, for example, the entire reactivity is by OH^- abstraction to form initially RCO^+, where R = H and CH_3, respectively. With HCO_2H, the ion product of the dominant (85%) channel, $HSOH^+$, indicates internal proton transfer from the formyl cation (HCO^+) to the HSO or HOS abstraction products before dissociation of the activated complex. With $C_2H_5CO_2H$, the OH^- abstraction channel comprises 50% of the ion product, with most of the remaining ion product (43%; see Table 2) accounted for by channel 14b, which forms $C_2H_5^+$ rather than HCO^+, due to the much lower proton affinity of CO.[63] The other, very minor, ion products with $C_2H_5CO_2H$ include $C_2H_4^+$ (formation of CO^+ is energetically unreasonable);[53,54] $m/z = 73$, which is most likely an H^- abstraction; $m/z = 60$, which is most reasonably $C_2H_4S^+$; and $m/z = 59$, which is most likely an isomer of $C_2H_3O_2^+$. Small signals from other possible ion products, such as $HSOH^+$ at $m/z = 50$, were observed but are not reported here due to the uncertainty of whether they arise from reactions with contaminant molecules or with $C_2H_5CO_2H$ (this is a particularly sticky gas with a low vapor pressure, which exacerbates the problem in this case).

Consistent with the above situation for the carboxylic acids, the reactions of the two acetate esters, CH_3CO_2R', and the two propionate esters, $C_2H_5CO_2R'$ (R′ = CH_3, C_2H_5), are dominated by the channels forming CH_3CO^+ and $C_2H_5CO^+$, respectively, although the reaction with methyl propionate has numerous other important channels (see Table 2). The two formate esters, however, do not react principally to form HCO^+, presumably because CO has a low proton affinity,[63] and therefore HCO^+ is not particularly stable compared to RCO^+ (R = CH_3, C_2H_5). Instead, the dominant ion product with HCO_2CH_3 is CH_2OH^+, implying association of the sulfur with the formyl group rather than the methoxy group; note that cleavage of the acyl−oxygen bond is again the principal mode of reaction. Channel 15b with HCO_2CH_3 forms an isomer of CH_4SO^+, which is likely either CH_3SOH^+ (as written in Table 2) or CH_3OSH^+. The neutral fragment in channel 15b is constrained to be CO by the reaction energetics, which implies that reaction proceeds via an ester bond cleavage, followed by internal proton transfer from the HCO^+ fragment to the CH_3SO or CH_3OS fragment prior to decomposition of the reaction complex. The ion product in channel 15d could be a mixture of SO^+ and CH_3SH^+, as occurs in the reaction with CH_3CHO (see above); however, SO^+ is chosen in Table 2 because a secondary ion product at $m/z = 80$ is observed, due most likely to CH_3OSOH^+ arising from the reaction of SO^+ with HCO_2CH_3.[23] The dominant channel with $HCO_2C_2H_5$ is $HSOH^+$, which implies that the neutral fragments are C_2H_4 and CO rather than C_2H_4CO; the latter molecule (methylketene), if formed, would likely show up in the product spectrum in protonated form as the highly stable $C_2H_5CO^+$ at $m/z = 57$, which is not observed. The ion product of channel 16b, which is more likely $C_2H_5^+$ than HCO^+, provides further evidence for this conclusion, since it can be interpreted in terms of a competition between HSO/HOS and C_2H_4 for a proton.

With the methyl and ethyl esters, several product channels occur in addition to the dominant ones forming RCO^+ (R = CH_3, C_2H_5). In many of these channels, the multitude of conceivable neutral products precludes their identification with certainty, and the choices indicated in Table 2 must be regarded as informed guesswork. In some cases, nonetheless, the implied neutral products are almost certain. For example, in channels 17b and 19c, the ion products imply OH^- abstraction to form HSO or HOS, which has been observed with many other reactions in the present study (see Table 2). Similarly, the O^- abstractions in channels 17f and 19h unequivocally form SO as the neutral product, and the neutral products of simple charge transfer and H^- abstraction are also unequivocal. An ion product appearing at $m/z = 59$ occurs with most of the esters, achieving its greatest prominence with the methyl esters, RCO_2CH_3 (R = CH_3, C_2H_5). With these, the most logical identity for this ion product is the methoxycarbonyl cation, $CH_3O-C^+{=}O$, which has appropriate connectivity and is a stable isomer of $[H_3,C_2,O_2]^+$.[66,67] Note that the complementary channel, in which the charge resides with the sulfurated species, appears with both methyl esters (see Table 2, channels 17d and 19b). The isomeric identity of $[H_3,C_2,O_2]^+$ is less certain where it appears as a very minor product with the ethyl esters and with propionic acid (see Table 2, channels 14f, 16e, 18e, and 20g). In general, the reactivities of methyl acetate and methyl propionate with $S^+(^4S)$ are similar, as are the reactivities of ethyl acetate and ethyl propionate (see Table 2). An ion product at $m/z = 60$, most likely an isomer of $C_2H_4S^+$ appears with all of the acids and esters for which R or R′ = C_2H_5, and the unequivocal product $C_2H_4^+$ appears with all of the propionic acids and esters. Space does not here permit more in-depth discussions of these extensively branched reactions of $S^+(^4S)$ with simple esters.

3.2. Comparison of the Reactivities of $S^+(^4S)$ and of $SO^+(X^2\Pi_r)$. The diatomic ion $SO^+(X^2\Pi_r)$ is closely coupled to $S^+(^4S)$ in ISC by reaction 2, and also by the dissociative electron/ion recombination:[22]

$$SO^+ + e \rightarrow S + O \qquad (6)$$

which cycles back to $S^+(^4S)$ through ionization of atomic $S(^3P)$ by cosmic rays or charged particles, such as C^+ (reaction 6 has not yet been studied in the laboratory).[22] Moreover, $SO^+(X^2\Pi_r)$ is strongly polar, with a Mullikan population of 0.693 on the S atom and 0.307 on the O atom,[68] and has a RE (=10.29 eV)[53] very close to that of $S^+(^4S)$ (=10.36 eV).[53] Thus, where reactivity is controlled by the charge site and the recombination energy, the reactivity of $SO^+(X^2\Pi_r)$ is expected to be very similar to that of $S^+(^4S)$. On the other hand, because $S^+(^4S)$ is atomic, somewhat smaller, and has more unpaired valence electrons than $SO^+(X^2\Pi_r)$, and because the enthalpy of formation of $S^+(^4S) + {}^1/_2\, O_2$ is 66.5 kcal mol^{-1} greater than that of $SO^+(X^2\Pi_r)$,[53] $S^+(^4S)$ is also expected to have additional modes of reactivity not available to $SO^+(X^2\Pi_r)$. Finally, the diatomic $SO^+(X^2\Pi_r)$ can react by rupture of the S−O bond to form separate S-bearing and O-bearing products, a mode of reactivity not available to $S^+(^4S)$. With the above considerations, it is interesting to compare the reactivities of these two ions where both of their reactions with a neutral molecule have been studied.

Table 3 presents such a comparison of the reactions of $S^+(^4S)$ and $SO^+(X^2\Pi_r)$ with 15 molecules from the present and former[1,13,23] studies. The product channels are classified mechanistically according to the key given in the table footnotes. Generally, reaction with both ions is efficient; exceptions are CH_4, with which $SO^+(X^2\Pi_r)$ does not react, and the low-atomicity OCS and CH_2O, with which it reacts significantly more slowly than does $S^+(^4S)$. The dominant product channels are strikingly similar for the two ions in many of these reactions, with $S^+(^4S)$ having a higher tendency for extensive product branching. Abstraction of H^- ("HAb") and OH^- ("HOAb") occupy the same product ranking for both ions in almost every reaction presented, although hydroxide abstraction is slightly more prominent for $S^+(^4S)$. Hydride abstraction followed by internal proton transfer ("HAb+P") is less prominent for $S^+(^4S)$ than for $SO^+(X^2\Pi_r)$, which is likely due to the lower proton affinity of HS than that of HSO.[28,56,63] "HOAb+P" is comparable for both ions. Charge transfer ("CT") is slightly more prominent for $S^+(^4S)$; an exception occurs with $CH_3C(O)CH_3$ (see Table 3). With HCO_2CH_3, CH_2OH^+ is the dominant ion product in both cases, with the next most prominent channel being abstraction of the methoxy (CH_3O) group with internal proton transfer ("MyAb+P").

Three essential differences in reactivity are observed. First, insertion of the ion into the neutral molecule, with ejection of a small neutral fragment (i.e., H, OH, or CH_3), is a rather common mode of reaction for $S^+(^4S)$, whereas it is extremely rare for $SO^+(X^2\Pi_r)$ (occurring only in a small channel with CH_2CHCH_3; see Table 3). Second, with the smaller saturated hydrocarbons (C_2H_2, C_2H_4, and CH_2CHCH_3 to a lesser extent), $SO^+(X^2\Pi_r)$ reacts principally by rupture of the S−O bond and a C−C bond to form products with S−C and O−C connectivities. Such behavior is, of course, impossible for $S^+(^4S)$, which reacts generally by insertion instead. Finally, $S^+(^4S)$ forms a greater wealth of products, except in the reactions with small, saturated hydrocarbons. Abstraction of CH_3 to form CH_3S^+ or CH_2SH^+ ("MeAb(+)") is particularly common with $S^+(^4S)$ but does not occur with $SO^+(X^2\Pi_r)$, although "MeAb" does occur in two of the reactions of $SO^+(X^2\Pi_r)$ (see Table 3). Abstraction of O and O^- ("OAb(+)" and "OAb," respectively) are also more prevalent for $S^+(^4S)$. Abstraction of CH_2 to form CH_2S^+ is a frequent, although always minor, product channel for $S^+(^4S)$, whereas it does not appear in the reactions of $SO^+(X^2\Pi_r)$. The appearance of insertion channels and additional product channels in the reactions of $S^+(^4S)$ are probably indicative of its greater enthalpy of formation, which can drive a greater variety of reaction modes. The higher spin-multiplicity of $S^+(^4S)$ may also play a role in its additional reactivity. The bond-rupture reactions of $SO^+(X^2\Pi_r)$ are necessarily distinct from any reactions that $S^+(^4S)$ can undergo.

4. Summary and Conclusions

The reactions of ground-state atomic $S^+(^4S)$ with 20 organic molecules containing oxygen or sulfur have been studied with a SIFT. Eighteen of these reactions are reported for the first time, and the remaining two (i.e., with CH_3SH and CH_2O) show significant differences in their rate coefficients and product distributions from the previously reported much earlier values.[12,13,18] The reactions of $S^+(^4S)$ with all 20 of these molecules are efficient, with bimolecular rate coefficients $k_{exp}^{(2)} \geq {}^2/_3 k_{th}^{(2)}$, where $k_{th}^{(2)}$ is the theoretical capture rate coefficient calculated from the theory of Su and Chesnavich.[48] The reactions of $S^+(^4S)$ with many hydrocarbons are also efficient, as shown by a former study; thus, the high spin-multiplicity of $S^+(^4S)$ does not generally hinder its reactivity through poor correlation of reactant and product electronic states, implying that perhaps spin flipping is facile with these reactions.[1]

The prominence of the charge (electron)-transfer channel in the reactions of $S^+(^4S)$ with the 20 organic molecules of this study and the 14 hydrocarbons of the former study[1] correlates strongly with RE($S^+(^4S)$) − IE(M), where the M are these 34

TABLE 3: Comparison of the Reactivities of Ground-State $S^+(^4S)$ and Ground-State $SO^+(X^2\Pi_r)$ with Organic Molecules for Which Both Reactions Have Been Studied[a]

reactant	%	$S^+(^4S)$[b] (10.36)	$k_{\mathrm{exp}}^{(2)}$[c]	%	$SO^+(^2\Pi_r)$[b,d] (10.29)	$k_{\mathrm{exp}}^{(2)}$[c,d]
CH_4	95	InH	4.0(−10)		NR	<3(−13)
(12.51)	5	HCS^+	(ref 1)			
C_2H_6	70	HAb	9.9(−10)	80	HAb+P	1.3(−9)
(11.52)	25	MeAb(+)	(ref 1)	20	HAb	
	5	InH				
C_3H_8	90	HAb	1.1(−9)	98	HAb	1.4(−9)
(10.95)	10	MeAb(+)	(ref 1)	2	HAb+P	
C_2H_2	100	InH	9.5(−10)	60	CH_2S^+	1.2(−9)
(11.40)			(ref 1)	22	HCS^+	
				17	CH_2CO^+	
				1	HCO^+	
C_2H_4	70	InMe	9.8(−10)	60	CH_2SH^+	1.1(−9)
(10.51)	30	InH	(ref 1)	20	CH_2S^+	
				6	CH_2OH^+	
				4	CH_3CS^+	
				4	HCS^+	
				2	HAb+P	
				2	CH_3SH^+	
				1	HCO^+	
				1	AS	
CH_2CHCH_3	40	HAb	1.2(−9)	64	HAb	1.3(−9)
(9.73)	30	CT	(ref 1)	14	CT	
	10	HCS^+		13	C_2H_5+	
	10	CH_2S^+		4	InOH	
	5	InMe		2	CH_3CO^+	
	5	InH		2	HCS^+	
				1	$C_3H_4S^+$	
CH_3OH	50	HAb	1.8(−9)	90	HAb	2.2(−9)
(10.84)	17	MeAb(+)		10	HAb+P	
	12	InH				
	12	OAb(+)				
	3	HOAb				
	2	CH_2S^+				
	2	HAb+P				
	2	HOAb(+)				
C_2H_5OH	53	HOAb	2.2(−9)	65	HOAb	2.3(−9)
(10.48)	22	HAb		15	HOAb+P	
	13	HOAb+P		15	HAb	
	7	InMe		5	MeAb	
	5	MeAb				
CH_3OCH_3	40	HAb	1.8(−9)	90	HAb	1.8(−9)
(10.03)	35	CT		10	CT	
	20	InMe				
	3	HOAb				
	2	MyAb				
OCS	100	S_2^+	9.1(−10)	55	S_2^+	4.9(−10)
(11.13)			(ref 13)	45	S_2O^+	
CH_2O	65	HAb	1.9(−9)	50	HAb	1.3(−9)
(10.88)	35	HAb+P		49	HAb+P	
				1	AS	
CH_3CHO	30	HAb	3.3(−9)	100	HAb	3.0(−9)
(10.23)	∼20	MeAb+P				
	∼15	OAb(+)				
	8	HOAb+P				
	8	CT				
	7	MeAb(+)				
	5	OAb				
	3	MeAb				
	2	InOH				
	2	CH_2S^+				
$CH_3C(O)CH_3$	65	HOAb	3.3(−9)	45	CT	2.8(−9)
(9.70)	15	MeAb		36	HOAb	
	14	CT		15	MeAb	
	4	OAb		2	OAb	
	2	$C_2H_5^+$		2	C_2H_5+	
HCO_2H	85	HOAb+P	1.7(−9)	85	HOAb+P	1.5(−9)
(11.33)	15	HOAb		10	HOAb	
				5	HAb+P	
HCO_2CH_3	30	CH_2OH^+	1.8(−9)	55	CH_2OH^+	2.1(−9)
(10.84)	20	MyAb+P		30	MyAb+P	
	13	MeAb(+)		15	HAb+P	
	10	OAb(+)				
	9	HAb+P				
	8	CH_2SO^+				
	5	MyAb(+)				
	3	MyAb				
	2	CH_2S^+				

[a] Recombination energies of the ions (eV) and first ionization energies of the neutral molecules (eV) are indicated in parentheses below the corresponding reactant. Also indicated are product percentages (%) for each product channel and experimentally measured bimolecular rate coefficients ($k_{\mathrm{exp}}^{(2)}$) for each reaction. [b] Ion product channels are classified by reaction type according to the following key: XAb = abstraction formally of the group X^- ; XAb+P = abstraction formally of the group X^-, followed by intramolecular proton (H^+) transfer; XAb(+) = abstraction formally of the group X; AS = ternary association; CT = charge transfer; InX = insertion of the ion followed by elimination of the group X; Me = CH_3; My = CH_3O; NR = no reaction. Other ion product channels are indicated by the observed ion product. [c] Experimentally determined binary reaction rate coefficients are presented in units of cm^3 $molecule^{-1}$ s^{-1}. Data for $S^+(^4S)$ not generated in the present study are obtained from the references indicated below the listed rate coefficients. [d] Reaction rate coefficients and product distributions for the reactions of $SO^+(^2\Pi_r)$ are taken from ref 23.

molecules.[28] Because the quantity $RE(S^+(^4S)) - IE(M) \leq 40$ kcal mol^{-1} for all 34 molecules, which is insufficient to break any of the covalent bonds occurring in these molecules, simple charge transfer (i.e., electron-jump) is always nondissociative. Therefore, the branching fractions, *f*, for the charge-transfer channels represent the total contributions from charge transfer.

Product channels other than charge transfer are quite varied, and with the 20 molecules in the present study, the primary ion product spectrum is often distributed among several substantial reaction channels. Again, because $RE(S^+(^4S)) - IE(M) \leq 40$ kcal mol^{-1} for these molecules, product formation generally occurs by reorganization of bonding arrangements rather than fragmentation. Although several different types or modes of reactivity are discernible (e.g., H^- abstraction, OH^- abstraction, insertion, etc.), their relative prominence as indicated by their branching fractions varies widely with the different neutral reactants. The reactions of $S^+(^4S)$ and those of $SO^+(^2\Pi_r)$, another important interstellar ion that is closely coupled to S^+ chemically in interstellar clouds, have many similar products with the molecules in the present and the former[1,23] studies. In general, the reactivities of $S^+(^4S)$ and $SO^+(^2\Pi_r)$ show that these ions can rapidly convert the wide variety of organic molecules observed in ISC into an even wider variety of other species, including neutral radicals, many of which have not yet been identified in ISC. To determine in detail the chemical evolution of sulfur compounds in ISC will require numerical chemical modeling, which is beyond the scope of the present work. However, particularly significant among the products are the isomeric radicals $HSO^\bullet$ and $SOH^\bullet$, which should be included in searches for new interstellar species.

Acknowledgment. The National Science Foundation, Division of Astronomical Sciences, is gratefully acknowledged for funding this work under grant AST-9415485. We also thank Pat Thaddeus of the Harvard-Smithsonian Center for Astrophysics for providing his most recent (March 1999) compilation of detected interstellar molecules,[25] and T. Daniel Crawford of the Center for Computational Quantum Chemistry at the University of Georgia for providing preliminary results of his cc-pVTZ/CCSD(T) computations on the [2H, S, O]$^+$ potential energy surface.

References and Notes

(1) Smith, D.; Adams, N. G.; Giles, K.; Herbst, E. *Astron. Astrophys.* **1988**, *200*, 191.
(2) Millar, T. J.; Herbst, E. *Astron. Astrophys.* **1990**, *231*, 466.
(3) Herbst, E.; Leung, C. M. *Mon. Not. R. Astron. Soc.* **1986**, *222*, 689.
(4) Herbst, E.; Leung, C. M. *Astrophys. J.* **1986**, *310*, 378.
(5) Smith, D. *Chem. Rev.* **1992**, *92*, 1473.
(6) Saito, S.; Kawaguchi, K.; Yamamoto, S.; Ohishi, M.; Suzuki, H.; Kaifu, N. *Astrophys J. Lett.* **1987**, *317*, L115.
(7) Yamamoto, S.; Saito, S.; Kawaguchi, K.; Kaifu, N.; Suzuki, H.; Ohishi, M. *Astrophys. J. Lett.* **1987**, *317*, L119.
(8) Wlodek, S.; Bohme, D. K.; Herbst, E. *Mon. Not. R. Astron. Soc.* **1988**, *235*, 493.
(9) Barrientos, C.; Largo, A. *J. Phys. Chem.* **1992**, *96*, 5808; Sumathi, R.; Peyerimhoff, S. D.; Sengupta, D. *J. Phys. Chem. A* **1999**, *103*, 772.
(10) Zakouril, P.; Glosik, J.; Skalsky, V.; Lindinger, W. *J. Phys. Chem.* **1995**, *99*, 15890.
(11) Petrie, S. *Mon. Not. R. Astron. Soc.* **1996**, *281*, 666.
(12) Anicich, V. G. *J. Phys. Chem. Ref. Data* **1993**, *22*, 1469.
(13) Ikezoe, Y.; Matsuoka, S.; Takebe, M.; Viggiano, A. *Gas-Phase Ion Molecule Reaction Rate Constants through 1986*; Maruzen Company, Ltd.: Tokyo, 1987.
(14) Smith, D.; Adams, N. G.; Lindinger, W. *J. Chem. Phys.* **1981**, *75*, 3365.
(15) Tichy, M.; Rakshit, A. B.; Lister, D. G.; Twiddy, N. D.; Adams, N. G.; Smith, D. *Int. J. Mass Spectrom. Ion Phys.* **1979**, *29*, 231.
(16) Stowe, G. F.; Schultz, R. H.; Wight, C. A.; Armentrout, P. B. *Int. J. Mass Spectrom. Ion Processes* **1990**, *100*, 177.
(17) Dzidic, I.; Good, A.; Kebarle, P. *Can. J. Chem.* **1970**, *48*, 664.
(18) Ruska, W. E. W.; Franklin, J. L. *Int. J. Mass Spectrom. Ion Phys.* **1969**, *3*, 221.
(19) Herbst, E. *Annu. Rev. Phys. Chem.* **1995**, *46*, 27.
(20) Dalgarno, A. *J. Chem. Soc., Faraday Trans.* **1993**, *89*, 2111.
(21) Turner, B. E. *Astrophys. J.* **1994**, *430*, 727.
(22) Turner, B. E. *Astrophys. J.* **1996**, *468*, 694.
(23) Decker, B. K.; Adams, N. G.; Babcock, L. M. R. R. Squires Memorial Issue. *Int. J. Mass Spectrom.*, in press.
(24) Prasad, S. S.; Huntress, W. T., Jr. *Astrophys. J.* **1982**, *260*, 590.
(25) McCarthy, M. C. In *Stellar Evolution, Stellar Explosions and Galactic Chemical Evolution*; Mezzacappa, A., Ed.; IOP Publishing: Ltd.: Philadelphia, 1998; p 205. A more recent, unpublished, list of detected interstellar molecular species compiled in March 1999 indicates 124 such species (including acetic acid, CH_3CO_2H, which does not appear in the McCarthy table) with no new sulfur-bearing species reported (Pat Thaddeus, personal communication).
(26) Geballe, T.; Oka, T. *Nature* **1996**, *384*, 334.
(27) McCall, B. J.; Geballe, T. R.; Hinkle, K. H.; Oka, T. *Science* **1998**, *279*, 1910.
(28) Adams, N. G.; Williams, T. L.; Babcock, L. M.; Decker, B. K. *Recent Res. Dev. Phys. Chem.* **1999**, *3*, 191.
(29) Bohme, D. K. In *Interaction Between Ions and Molecules*; Ausloos, P., Ed.; Plenum: New York, 1975; p 489.
(30) Turner, B. E.; Ziurys, L. M. In *Galactic and Extragalactic Radio Astronomy*, 2nd ed.; Verschuur, G. L., Kellermann, K. I., Eds.; Springer-Verlag: New York, 1988; p 200 and ff.
(31) Weinreb, S.; Barrett, A. H.; Meeks, M. L.; Henry, J. C. *Nature* **1963**, *200*, 829.
(32) Sofia, U. J.; Cardelli, J. A.; Savage, B. D. *Astrophys. J.* **1994**, *430*, 650.
(33) Trimble, V. *Rev. Mod. Phys.* **1975**, *47*, 877.
(34) Palumbo, M. E.; Geballe, T. R.; Tielens, A. G. G. M. *Atrophys. J.* **1997**, *479*, 839.
(35) Caselli, P.; Hasegawa, T. I.; Herbst, E. *Astrophys. J.* **1993**, *408*, 548.
(36) Millar, T. J.; Herbst, E.; Charnley, S. B. *Astrophys. J.* **1991**, *369*, 147.
(37) Charnley, S. B. *Astrophys. J.* **1997**, *481*, 396.
(38) Decker, B. K.; Adams, N. G. *Int. J. Mass Spectrom. Ion Processes* **1997**, *165/166*, 257.
(39) Decker, B. K.; Adams, N. G.; Babcock, L. M. *Int. J. Mass Spectrom.* **1999**, *185/186/187*, 727.
(40) Adams, N. G.; Smith, D. In *Techniques for the Study of Ion−Molecule Reactions*; Farrar, J. M., Saunders, W. H., Eds.; Wiley: New York, 1988; p 165.
(41) Yaws, C. L. *Handbook of Viscosity*; Library of Physico-Chemical Property Data; Gulf Publishing Company: Houston, 1995.
(42) Taylor, M. D. *J. Am. Chem. Soc.* **1951**, *73*, 315.
(43) Taylor, M. D.; Bruton, J. *J. Am. Chem. Soc.* **1952**, *74*, 4151.
(44) Adams, N. G.; Smith, D. *Int. J. Mass Spectrom. Ion Phys.* **1976**, *21*, 349.
(45) Adams, N. G.; Smith, D. *J. Phys. B* **1976**, *9*, 1439.
(46) Emsley, J. *The Elements*; Clarendon Press: Oxford, U.K., 1990.
(47) Radzig, A. A.; Smirnov, B. M. *Reference Data on Atoms, Molecules, and Ions*; Springer-Verlag: Berlin, 1985; p 262.
(48) Su, T.; Chesnavich, W. J. *J. Chem. Phys.* **1982**, *76*, 5183.
(49) Lide, D. R., Ed. *CRC Handbook of Chemistry and Physics*, 78th ed.; CRC Press: Boca Raton, FL, 1997.
(50) Dean, J. A., Ed. *Lange's Handbook of Chemistry*, 14th ed.; McGraw-Hill: New York, 1992.
(51) Clary, D. C.; Smith, D.; Adams, N. G *Chem. Phys. Lett.* **1985**, *119*, 320.
(52) Adams, N. G.; Smith, D.; Clary, D. C. *Astrophys. J.* **1985**, *296*, L31.
(53) Mallard, W. G.; Linstrom, P. J., Eds. *NIST Webbook*; NIST Standard Reference Database Number 69; National Institute of Standards and Technology: Gaithersburg, November 1998; http://webbook.nist.gov.
(54) Lias, S. G.; Bartmess, J. E.; Liebman, J. F.; Holmes, J. L.; Levin, R. D.; Mallard, W. G. *NIST Positive Ion Energetics*, Version 1.1; National Institute of Standards and Technology: Gaithersburg, MD, January 1990.
(55) Xantheas, S. S.; Dunning, T. H., Jr. *J. Phys. Chem.* **1993**, *97*, 6616.
(56) Decker, B. K.; Adams, N. G.; Babcock, L. M.; Crawford, T. D.; Schaefer, H. F., III. *J. Am. Chem. Soc.*, submitted for publication.
(57) Ruscic, B.; Berkowitz, J. *J. Chem. Phys.* **1991**, *95*, 4033.
(58) Ruttink, P. J. A.; Burgers, P. C.; Francis, J. T.; Terlouw, J. K. *J. Phys. Chem.* **1996**, *100*, 9694.
(59) Gozzo, F. C.; Eberlin, M. N. *J. Mass Spectrom.* **1995**, *30*, 1553.
(60) Cheng, B.-M.; Eberhard, J.; Chen, W.-C.; Yu, C.-h. *J. Chem. Phys.* **1997**, *106*, 9727.
(61) McLafferty, F. W.; Turecek, F. *Interpretation of Mass Spectra*, 4th ed.; University Science Books: Mill Valley, CA, 1993; p 141.
(62) Nobes, R. H.; Radom, L. *Chem. Phys. Lett.* **1992**, *189*, 554.
(63) Hunter, E. P. L.; Lias, S. G. *J. Phys. Chem. Ref. Data* **1998**, *27*, 413.
(64) Although PA(SH) is not reported in Reference (62), it can be estimated as ~158 kcal mol^{-1} from the enthalpies of formation of H^+, SH, and H_2S^+, available in References (53) and (54). This is significantly greater than PA(CO) = 142 kcal mol^{-1}, from Reference (63).
(65) Rice, B. M.; Chabalowski, C. F. *J. Phys. Chem.* **1994**, *98*, 9488.
(66) Blanchette, M. C.; Holmes, J. L.; Hop, C. E. C. A.; Lossing, F. P.; Postma, R.; Ruttink, P. J. A.; Terlouw, J. K. *J. Am. Chem. Soc.* **1986**, *108*, 7589.
(67) Sekiguchi, O.; Aoyagi, K.; Tajima, S.; Nibbering, N. M. M. *J. Mass Spectrom.* **1997**, *32*, 755.
(68) Crawford, T. D. Private communication.